Supplementary Material for Relationship between Enthalpy Fluctuation and Nonexponential Relaxation in Glass-forming Liquids

W. Takeda[1] and P. Lucas[1]

[1] Department of Materials Science and Engineering, University of Arizona, Tucson, AZ 85712, United States

This supplementary material includes detailed derivation of Eq. 3 in the main text in Sec. I, the detailed fitting procedures for the heat capacities of the three systems as well as the fitting parameters in Sec. II, the method of calculating S_c from ΔC_p for $Pd_{43}Cu_{27}Ni_{10}P_{20}$ and PVAc in Sec. III, the re-calculation procedure of $\sigma_{T_f^e}$ from ΔT_β for PVAc in Sec. IV, the detailed method for the fitting of $\sigma_{T_f^e}$ of $Pd_{43}Cu_{27}Ni_{10}P_{20}$ in Sec. V, and the reported β_{KWW}, ΔT_β, and $\sigma_{T_f^e}$ values used in the main text in Sec. VI.

I. Derivation of DFDT Equation

The fluctuation in relaxation time in equilibrium is proportional to the small equilibrium fictive temperature fluctuation of i-th domain $\delta T_{f,i}^e$ as

$$\ln \tau_i\,(T) = \langle \ln \tau\,(T + \delta T_{f,i}^e \rangle, \tag{s1}$$

The first-order Taylor expansion of Eq. s1 around its mean yields

$$\ln \tau_i\,(T) = \langle \ln \tau \rangle + \left(\frac{\partial \langle \ln \tau(T) \rangle}{\partial T}\right) \delta T_{f,i}^e, \tag{s2}$$

Thus, the relaxation time fluctuation of i-th domain, $\delta \ln \tau_i$, is

$$\delta \ln \tau_i = \ln \tau_i\,(T) - \langle \ln \tau \rangle = \left(\frac{\partial \langle \ln \tau(T) \rangle}{\partial T}\right) \delta T_{f,i}^e. \tag{s3}$$

Then, the variance (fluctuation) of log-relaxation time becomes

$$\sigma_{\ln \tau}^2 = \langle (\delta \ln \tau_i)^2 \rangle = \left(\frac{\partial \langle \ln \tau(T) \rangle}{\partial T}\right)^2 \langle \left(\delta T_{f,i}^e\right)^2 \rangle, \tag{s4}$$

where $\langle \left(\delta T_{f,i}^e\right)^2 \rangle$ is the variance of equilibrium fictive temperature $\sigma_{T_f^e}$. Substituting $\langle \left(\delta T_{f,i}^e\right)^2 \rangle$ to $\sigma_{T_f^e}$ in Eq. s4, and solving it for $\sigma_{T_f^e}$ gives

$$\sigma_{T_f^e} = \frac{\sigma_{\ln \tau}}{\left|\frac{\partial \langle \ln \tau(T) \rangle}{\partial T}\right|}. \tag{s5}$$

Eq. s5 is Eq. 3 in the main text.

II. Heat capacities of B_2O_3, PVAc, and $Pd_{43}Cu_{27}Ni_{10}P_{20}$

Heat capacity data are taken from Ref.[1] for B_2O_3, Ref.[2] for $Pd_{43}Cu_{27}Ni_{10}P_{20}$, and Ref.[3] for PVAc. We fit the heat capacity of solid (glass or crystal) and that of liquid by empirical equations to obtain $\Delta C_p(T)$.

For B_2O_3 and PVAc, the heat capacity of glass C_p^g is fitted by the semi-empirical formula of Tsao[4]:

$$C_p^g(T) = \frac{T^2}{T^2 + \theta^2}(c_0 + c_1 T), \tag{s6}$$

where θ, c_0 and c_1 are the fitting parameters. For $Pd_{43}Cu_{27}Ni_{10}P_{20}$, we used the empirical formula and obtained parameters shown in Ref.[5] for the heat capacity of crystalline phase C_p^c. The formula is

$$C_p^c(T) = 3R_{Gas} + c_2 T + c_3 T^2, \tag{s7}$$

where R_{Gas} is a universal gas constant, c_2 and c_3 are the fitting parameters. The heat capacity of liquid C_p^l for B_2O_3 is assumed to be constant, 8.314 J/(mol·K), and that for PVAc is assumed to follow a linear function as:

$$C_p^l(T) = c_4 + c_5 T. \tag{s8}$$

The formula for C_p^l of $Pd_{43}Cu_{27}Ni_{10}P_{20}$ is taken from Gallino *et al.*[5] as

$$C_p^l(T) = 3R_{Gas} + c_6 T + \frac{c_7}{T^2}, \tag{s9}$$

where c_6 and c_7 are the fitting parameters. All the fitting parameters used for the heat capacity are summarized in Table s1, and the fitted lines for all three systems are shown in Fig. s1.

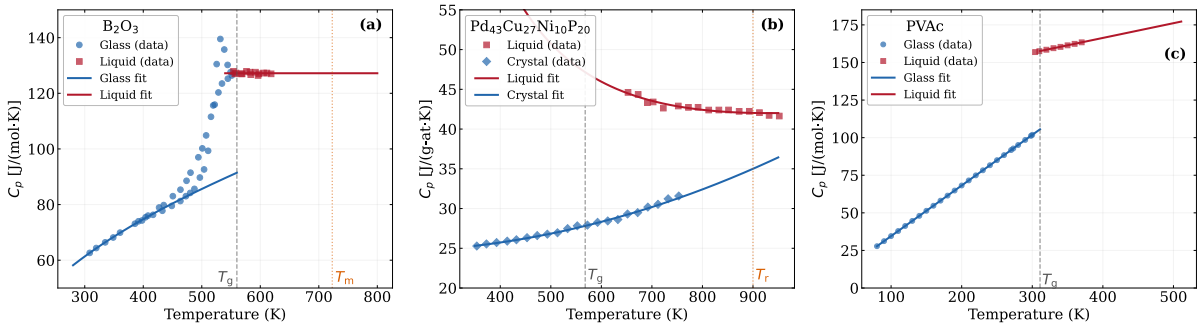

FIG s1. Heat capacities of the three systems investigated in the main text. (a) is for B_2O_3 from Ref.[1], (b) is for $Pd_{43}Cu_{27}Ni_{10}P_{20}$ from Ref.[2], and (c) is for PVAc from Ref.[3]

Table s1. Heat capacity fitting parameters for the three glass-forming systems. In Eq. s6, θ is in K, c_0 in J/(mol·K), and c_1 in J/(mol·K²). In Eq. s7, c_2 is in J/(mol·K²) and c_3 in J/(mol·K³). In Eq. s8, c_4 is in J/(mol·K), c_5 in J/(mol·K²). In Eq. s9, c_6 in J/(mol·K²), and c_7 in J·K/mol. R_{Gas} = 8.314 J/(mol·K).

System	Phase	Model	Parameters
B_2O_3	Glass	Eq. s6	$\theta = 168.0$, $c_0 = 58.58$, $c_1 = 0.07338$
B_2O_3	Liquid	Constant	127.21
$Pd_{43}Cu_{27}Ni_{10}P_{20}$	Crystal	Eq. s7	$c_2 = -5.411 \times 10^{-3}$, $c_3 = 1.843 \times 10^{-5}$

$Pd_{43}Cu_{27}Ni_{10}P_{20}$	Liquid	Eq. s9	$c_6 = 1.2224 \times 10^{-2}$, $c_7 = 4.9269 \times 10^6$
PVAc	Glass	Eq. s6	$\theta = 1.0$, $c_0 = 0.88$, $c_1 = 0.33658$
PVAc	Liquid	Eq. s8	$c_4 = 127.12$, $c_5 = 0.09802$

III. Calculation of S_c from ΔC_p for $Pd_{43}Cu_{27}Ni_{10}P_{20}$and PVAc

As for B_2O_3, we assume that the configurational entropy can be approximated by the excess entropy, $S_c \approx S_{ex}$.

For $Pd_{43}Cu_{27}Ni_{10}P_{20}$, the configurational entropy is anchored at a reference temperature T_r above the liquidus, where $S_c(T_r)$ is known from thermodynamic integration of calorimetric data following the procedure used by Gallino *et al.*[5] The configurational entropy at lower temperatures is obtained by integrating downward from T_r:

$$S_c(T) \approx S_{ex}(T) = S_c(T_r) - \int_T^{T_r} \frac{\Delta C_p(T')}{T'} dT', \tag{s10}$$

where $\Delta C_p = C_p^l - C_p^c$, $T_r = 900$ K, and $S_c(T_r) = 11.26\ \mathrm{J/(mol \cdot K)}$. Here, the crystal heat capacity is used as the vibrational baseline in place of the glass heat capacity, following the convention for metallic glass-forming liquids where a well-defined crystalline phase exists[6].

For PVAc, no melting transition is observed, so the configurational entropy is anchored at the Kauzmann temperature T_K, where $S_c(T_k) = 0$ by definition. The configurational entropy is then obtained by integrating upward from T_k:

$$S_c(T) = \int_{T_k}^{T} \frac{\Delta C_p(T')}{T'} dT', \tag{s11}$$

where $C_p = C_p^l - C_p^g$, and we assumed the Vogel temperature determined from the dielectric spectroscopy is the same as the Kauzmann temperature, $T_K \approx T_v = 267$ K[7]. The obtained $S_c(T)$ is plotted in Fig. 3(a) in the main text.

IV. Re-calculation of $\sigma_{T_f^e}$ for PVAc using ΔT_β of Hallavant *et al.*

Hallavant *et al.* measured the width of the glass transition ΔT_β of PVAc during cooling for a wide range of cooling rate in Ref.[8]. The authors then used the following equation to obtain the temperature fluctuation (equivalently, $\sigma_{T_f^e}$ in the current manuscript) as

$$\sigma_{T_f^e} = \frac{\Delta T_\beta}{2\kappa}, \tag{s12}$$

where κ is the vitrification function first introduced by Schawe in Ref.[9].

We find that $\sigma_{T_f^e}$ values for PVAc reported in Ref.[8] are systematically overestimated when compared with the $\sigma_{T_f^e}$ values reported by Tombari *et al.*[10] and Hempel *et al.*[11], which were measured using M-DSC. Thus, we re-calculate $\sigma_{T_f^e}$ from the reported ΔT_β by Hallavant *et al.* using Eq. s12. Fig. s2 compares these re-calculated values (thick green diamonds) with the originally reported $\sigma_{T_f^e}$ from Ref.[8] (thin green diamonds) and the measured values by Tombari *et al.*[10] (blue circle) and Hempel *et al.*[11] (red square). The re-calculated $\sigma_{T_f^e}$ is obtained by combining a linear fit to the Tombari and Hempel data with the ΔT_β values from Hallavant *et al.*[8].

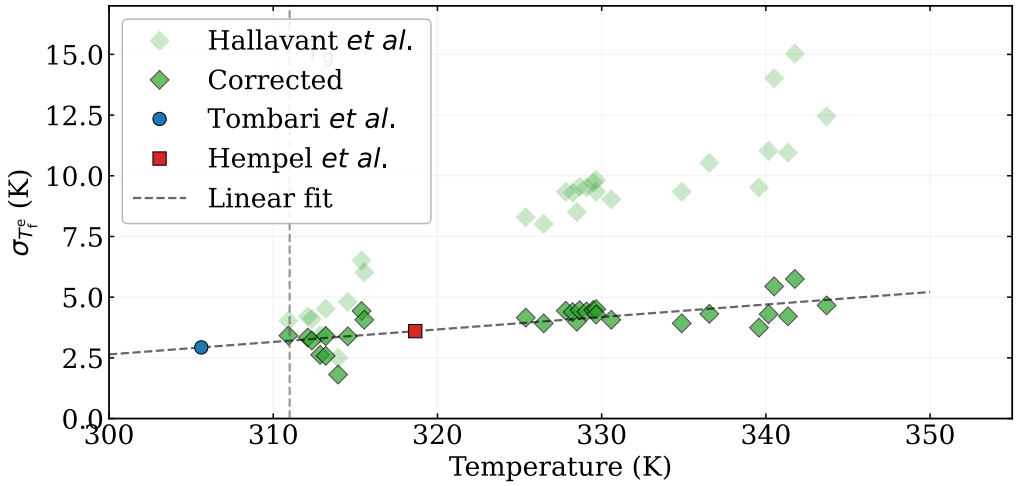

FIG s2. Equilibrium fictive-temperature fluctuations in PVAc. The thin green diamonds show the measured $\sigma_{T_f^e}$ reported by Hallavant *et al.* using FSC[8]; the blue circle shows the values measured by Tombari *et al.*[10]; and the red square shows the values reported by Hempel *et al.*[11] by using M-DSC. The dashed line is the linear fit to Tombari and Hempel dataset. The thick green diamonds indicate the re-calculated $\sigma_{T_f^e}$ values from Hallavant's dataset based on the linear fit using Eq. s12.

V. Fitting procedures for $\sigma_{T_f^e}$ of $Pd_{43}Cu_{27}Ni_{10}P_{20}$

In this section, we describe the fitting procedure for $\sigma_{T_f^e}$ of $Pd_{43}Cu_{27}Ni_{10}P_{20}$ shown in Fig. 4(b) in the main text. We found that the experimental $\sigma_{T_f^e}$ data from Schawe *et al.*[12] are best described by two separate linear fits with a crossover near $T \approx 593$K. To capture this behavior, we used two separate linear models, one for each region, blended via a sigmoid function:

$$\sigma_{T_f^e}(T) = w(T)(c_8 + c_9 T) + \big(1 - w(T)\big)(c_{10} + c_{11} T), \qquad \text{(s13)}$$

where $w(T) = [1 + \exp((T - T_{\text{mid}})/\Delta T)]^{-1}$ is a sigmoid transition function that smoothly interpolates between the two linear regimes. The equilibrium fictive temperature fluctuation rate, $R(T) = T\, d(\ln \sigma_{T_f^e})/dT$, is then computed numerically from this blended function (see Fig. s3). The fitting parameters are listed in Table s2. Error bars on the $R(T)$ represent 95% confidence intervals from the linear fits.

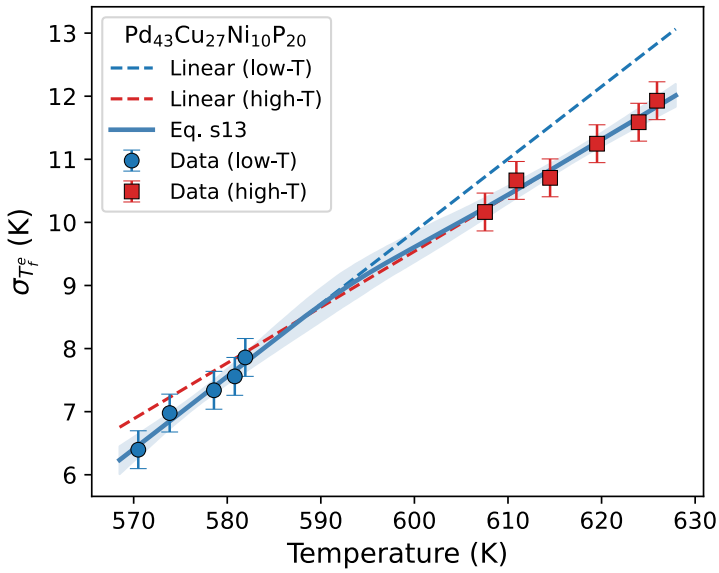

FIG s3. Fitted $\sigma_{T_f^e}(T)$ for $Pd_{43}Cu_{27}Ni_{10}P_{20}$ using Eq. s13. Markers and lines are described in the legend. The blue shaded region is the 95% confidence envelope.

Table s2. Two-region linear fit parameters for $\sigma_{T_f^e}(T)$ of $Pd_{43}Cu_{27}Ni_{10}P_{20}$. c_8 and c_{10} are in K, c_9 and c_{11} are dimensionless K/K. T_{mid} and ΔT are in K.

Parameter	Region 1 ($T < 593$ K)	Region 2 ($T \geq 593$ K)
T range [K]	570.49 to 581.93	607.54 to 625.92
Number of data points	5	6
c_8 or c_{10}	-59.11	-43.55
c_9 or c_{11}	0.1149	0.0885
R-squared	0.97	0.97
T_{mid} [K]	594.7	
ΔT [K]	4.0	

VI. Experimental nonexponential values for three systems

Here we summarize the experimental nonexponential values used in the main text. They are all taken from the literature.

B_2O_3 β_{KWW} Data

T [K]	β_{KWW}	Source
509.86	0.59	Sidebottom *et al.*[13]
518.31	0.58	"
523.47	0.54	"
529.11	0.55	"
531.46	0.70	"
535.21	0.73	"
542.25	0.68	"
558.69	0.59	"
591.55	0.65	"
600.00	0.60	"

626.29	0.67	″
653.52	0.73	″
670.42	0.71	″
673.24	0.74	″
684.98	0.71	″
694.84	0.68	″
727.23	0.72	″
743.66	0.81	″
769.95	0.86	″
543.87	0.52	Bartenev *et al.*[14]
504.45	0.49	″
509.09	0.52	″
524.16	0.48	″
517.21	0.50	″
529.96	0.50	″
541.56	0.50	″
550.83	0.50	″
560.11	0.50	″
570.54	0.50	″
495.18	0.50	″
565.90	0.55	″
577.50	0.55	″
587.93	0.55	″
608.80	0.60	″
663.29	0.65	″
685.32	0.64	″
727.06	0.70	″
802.43	0.80	″
829.09	0.85	″
972.86	0.85	″
1023.87	0.95	″
1074.89	0.95	″

PVAc β_{KWW} Data

T [K]	β_{KWW}	Source
306.76	0.47	Alegria *et al.*[7]
307.57	0.46	″
308.63	0.48	″
308.63	0.49	″
311.06	0.47	″
312.39	0.49	″
312.65	0.50	″
313.72	0.51	″
316.95	0.50	″
318.83	0.49	″
319.63	0.50	″

323.93	0.51	〃
328.74	0.53	〃
333.84	0.55	〃
338.94	0.55	〃
344.04	0.56	〃
349.14	0.57	〃
353.97	0.57	〃
359.34	0.58	〃
364.17	0.59	〃
369.54	0.59	〃
374.64	0.60	〃
379.20	0.62	〃
384.30	0.63	〃
389.41	0.62	〃
394.50	0.64	〃
399.61	0.62	〃
404.71	0.63	〃
409.82	0.62	〃
414.67	0.60	〃
419.77	0.60	〃
424.86	0.62	〃
429.70	0.62	〃
435.34	0.63	〃
440.15	0.66	〃
445.26	0.65	〃
450.09	0.66	〃
455.19	0.67	〃
460.30	0.67	〃
465.40	0.67	〃
470.49	0.69	〃
322.15	0.56	Sasabe *et al.*[15]
322.79	0.51	〃
325.98	0.56	〃
330.98	0.57	〃
336.09	0.58	〃
339.70	0.59	〃
344.38	0.59	〃
344.38	0.62	〃
349.81	0.60	〃
352.68	0.64	〃

$Pd_{43}Cu_{27}Ni_{10}P_{20}$ $\sigma_{T_f^e}$ Data (Schawe *et al.* in Ref.[12])

T [K]	$\sigma_{T_f^e}$ [K]
570.49	6.40
573.85	6.98
578.58	7.34

580.81	7.56
581.93	7.86
607.54	10.16
610.90	10.67
614.50	10.71
619.51	11.25
623.97	11.59
625.92	11.93

PVAc ΔT_β Data (Hallavant *et al.* in Ref.[8])

T [K]	ΔT_β [K]
310.92	11.29
312.10	11.78
312.35	11.49
312.86	9.63
313.19	12.66
313.19	9.64
313.95	7.00
314.54	13.44
315.38	18.23
315.55	16.86
325.38	23.22
326.47	22.44
327.82	26.15
328.49	23.81
328.24	26.06
328.66	26.74
329.08	26.64
329.50	27.23
329.66	27.52
329.66	26.16
330.59	25.28
334.87	26.17
336.55	29.49
339.58	26.66
340.17	30.86
340.50	39.25
341.34	30.67
341.76	42.08
343.70	34.87

References:

[1] S.B. Thomas, G.S. Parks, Studies on Glass. VI. Some Specific Heat Data on Boron Trioxide, J. Phys. Chem. 35 (1931) 2091–2102. https://doi.org/10.1021/j150325a016.

[2] M. Kuno, L.A. Shadowspeaker, J. Schroers, R. Busch, Thermodynamics of the Pd43Ni10Cu27P 20bulk metallic glass forming alloy, Materials Research Society

Symposium - Proceedings 806 (2003) 227–232. https://doi.org/10.1557/proc-806-mm5.2.

[3] U. Gaur, B.B. Wunderlich, B. Wunderlich, Heat Capacity and Other Thermodynamic Properties of Linear Macromolecules. VII. Other Carbon Backbone Polymers, J. Phys. Chem. Ref. Data 12 (1983) 29–63. https://doi.org/10.1063/1.555677.

[4] J.Y. Tsao, Two semiempirical expressions for condensed-phase heat capacities, J. Appl. Phys. 68 (1990) 1928–1930. https://doi.org/10.1063/1.346588.

[5] I. Gallino, J. Schroers, R. Busch, Kinetic and thermodynamic studies of the fragility of bulk metallic glass forming liquids, J. Appl. Phys. 108 (2010). https://doi.org/10.1063/1.3480805.

[6] H.L. Smith, C.W. Li, A. Hoff, G.R. Garrett, D.S. Kim, F.C. Yang, M.S. Lucas, T. Swan-Wood, J.Y.Y. Lin, M.B. Stone, D.L. Abernathy, M.D. Demetriou, B. Fultz, Separating the configurational and vibrational entropy contributions in metallic glasses, Nat. Phys. 13 (2017) 900–905. https://doi.org/10.1038/nphys4142.

[7] A. Alegría, J. Colmenero, P.O. Mari, I.A. Campbell, Dielectric investigation of the temperature dependence of the nonexponentiality of the dynamics of polymer melts, Phys. Rev. E Stat. Phys. Plasmas Fluids Relat. Interdiscip. Topics 59 (1999) 6888–6895. https://doi.org/10.1103/PhysRevE.59.6888.

[8] K. Hallavant, M. Mejres, J.E.K. Schawe, A. Esposito, A. Saiter-Fourcin, Influence of Chemical Composition and Structure on the Cooperative Fluctuation in Supercooled Glass-Forming Liquids, Journal of Physical Chemistry Letters 15 (2024) 4508–4514. https://doi.org/10.1021/acs.jpclett.4c00632.

[9] J.E.K. Schawe, Vitrification in a wide cooling rate range: The relations between cooling rate, relaxation time, transition width, and fragility, Journal of Chemical Physics 141 (2014) 184905. https://doi.org/10.1063/1.4900961.

[10] E. Tombari, C. Ziparo, G. Salvetti, G.P. Johari, Vibrational and configurational heat capacity of poly(vinyl acetate) from dynamic measurements, Journal of Chemical Physics 127 (2007). https://doi.org/10.1063/1.2747596.

[11] E. Hempel, G. Hempel, A. Hensel, C. Schick, E. Donth, Characteristic Length of Dynamic Glass Transition near Tg for a Wide Assortment of Glass-Forming Substances, Journal of Physical Chemistry B 104 (2000) 2460–2466. https://doi.org/10.1021/jp991153f.

[12] J.E.K. Schawe, M.K. Kwak, M. Stoica, E.S. Park, J.F. Löffler, The Cooperativity of Atomic Fluctuations in Highly Supercooled Glass-Forming Metallic Melts, Journal of Physical Chemistry Letters 16 (2025) 948–954. https://doi.org/10.1021/acs.jpclett.4c03275.

[13] D. Sidebottom, R. Bergman, L. Börjesson, L.M. Torell, Two-step relaxation decay in a strong glass former, Phys. Rev. Lett. 71 (1993) 2260–2263. https://doi.org/10.1103/PhysRevLett.71.2260.

[14] G.M. Bartenev, V.A. Lomovskoi, Relaxation time spectra and the peculiarities of the process of boron anhydride glass transition, J. Non. Cryst. Solids 146 (1992) 225–232. https://doi.org/10.1016/S0022-3093(05)80495-8.

[15] H. Sasabe, C.T. Moynihan, Structural Relaxation in Poly(Vinyl Acetate)., J Polym Sci Polym Phys Ed 16 (1978) 1447–1457. https://doi.org/10.1002/pol.1978.180160810.